Virtual Heat Flux Measurements from a Boundary-Layer Profiler–RASS Compared to Aircraft Measurements

WAYNE M. ANGEVINE AND S. K. AVERY

CIRES, University of Colorado/NOAA, Boulder, Colorado

G. L. KOK

NCAR Research Aviation Facility, Boulder, Colorado

(Manuscript received 1 March 1993, in final form 10 May 1993)

ABSTRACT

Measurements of the turbulent virtual heat flux in the convective atmospheric boundary layer made with a 915-MHz boundary-layer wind profiler–radio acoustic sounding system (RASS) are compared to flux measurements from a King Air aircraft. The profiler–RASS flux was calculated by a refined eddy correlation technique. The measurements were made during the Rural Oxidants in the Southern Environment II experiment in June 1992. The area over which the measurements were made is primarily pine forest, and the dominant weather conditions were hot with light winds. The profiler–RASS measurements and the aircraft measurements agree well. Even under these light wind conditions, a 2-h-average profiler–RASS measurement may be sufficiently accurate to be useful. The instrumental error is estimated to be less than the uncertainty due to sampling of the turbulence.

1. Introduction

In an earlier paper (Angevine et al. 1993) the authors reported preliminary work on the measurement of turbulent virtual heat flux in the convective atmospheric boundary layer with a boundary-layer profiler–radio acoustic sounding system (RASS). The primary question remaining from that work was whether the measured results would compare favorably with established techniques, particularly aircraft measurements. To answer that question, a profiler–RASS was included in the Rural Oxidants in the Southern Environment II (ROSE II) experiment near Jachin, Alabama, in June 1992. The King Air aircraft from the National Center for Atmospheric Research (NCAR) Research Aviation Facility made several research flights over the ROSE II site. A sonic anemometer operated by the Atmospheric Turbulence and Diffusion Division (ATDD) of the National Oceanic and Atmospheric Administration (NOAA) Air Resources Laboratory was on a tower just above the forest canopy near the profiler–RASS site.

The turbulent virtual heat flux is defined as

$$Q_v = \rho C_p \overline{w'T'_v}, \qquad (1)$$

where w' is the perturbation of vertical velocity, T'_v the perturbation of virtual temperature, ρ the density, and C_p the specific heat. It is proportional to the kinematic buoyancy flux $\overline{w'T'_v}$. The virtual heat flux is the primary driver of boundary-layer mixing under light wind conditions (Stull 1988, p. 155) and is therefore of interest in any boundary-layer observation or modeling program. The flux is calculated from the profiler–RASS data by eddy correlation, with refinements as discussed below.

The experiment site was within a managed pine forest. Sections of the forest had been cut and replanted at various times leaving a patchwork of various sizes of trees. The profiler–RASS was located in an area that had been cleared about four years before and had pine trees about 2 m high as well as other lower brush. Weather conditions were ideal during the period when the aircraft and surface instruments were operating (18–26 June 1992), with clear to partly cloudy skies and no significant rainfall.

The 915-MHz profiler was designed at the NOAA Aeronomy Laboratory (Ecklund et al. 1988) and is now commonly used for wind profiling in the boundary layer. A RASS is made up of a Doppler radar—in this case, the profiler—and one or more acoustic sources (Matuura et al. 1986; May et al. 1988; May et al. 1990). The acoustic sources are located near the radar antenna, and the radar measures the speed at which the acoustic wave propagates. The speed of sound is proportional to the square root of virtual temperature. If the air is moving along the beam, the apparent sound speed will

Corresponding author address: Wayne Angevine, NOAA Aeronomy Laboratory, R/E/AL3, 325 Broadway, Boulder, CO 80303.

be changed, so it is necessary to measure and correct for the radial wind velocity. With the recent addition of the capability to measure the radial wind velocity and acoustic velocity simultaneously when used as a RASS (Angevine et al. 1994), the components needed for eddy correlation flux measurements are available.

The profiler used in the ROSE II experiments operated at 915 MHz with a 1.8-m-square four-panel microstrip patch array antenna and 500 W of peak power. The one-way half-power beamwidth was 9°. The RASS acoustic power was 30 W. The antenna was mechanically steered into five beam positions: one vertical and four oblique positions 12° off zenith in two perpendicular planes. The oblique beam positions allowed the system to operate as a wind profiler as well as to measure the temperature profile and buoyancy flux. Both acoustic and radial wind velocities were measured in all beam positions. A large aluminum honeycomb clutter fence was used to prevent ground clutter from nearby trees.

2. Technique

a. Profiler operation and sampling

The profiler sampled each beam position for 30 s and then spent 10 s performing calculations and allowing the antenna to move and stabilize. Therefore a temperature profile was available every 40 s. The range resolution was 100 m and the lowest range gate was centered at 150 m. The profiler averages air motions and temperature in a resolution cell that is defined in the along-beam direction by the range resolution, in the direction along the wind by the product of wind velocity and sampling time, and in the crosswind direction by the beam width. For example, if the wind speed is 2 m s^{-1}, the resolution cell dimensions at 150-m range are 100 m vertical, 60 m (30 s $\times$ 2 m s^{-1}) along the wind, and 16 m crosswind.

b. Profiler data processing

The raw profiler–RASS data contain both good and bad estimates of the wind and acoustic velocities. Bad velocity estimates may be due to ground clutter, birds, insects, aircraft, poor return signal power, rain, or radio frequency interference. Before they can be used to calculate flux, the velocity time series must be cleaned to remove as many of the bad data points as possible. Traditional profiler data-cleaning algorithms rely on continuity in height and/or time to distinguish bad data from good. That is, good velocity estimates are taken to be those that are reasonably similar to estimates above, below, before, and after the particular height and time in question. In the turbulent convective boundary layer, this assumption is not generally valid. The size of the radar resolution cell is within the range of scales of active turbulence, and so individual measurements are expected to differ substantially even in adjacent heights and times.

The approach used on the data presented here is to test the data against statistical windows. The windows are applied to each of the parameters available from the profiler, that is, to the signal-to-noise ratio (SNR), the velocity, and the spectral width of the clear-air and acoustic velocity spectra. The data are divided into 2-h segments that contain about 180 individual measurements. Data points that fall within the following limits based on the mean, median, and standard deviation σ of the 2-h time series are considered "good":

clear-air velocity	median $\pm 3\sigma$;
clear-air spectral width	mean $\pm 2\sigma$;
clear-air SNR	mean $\pm 2\sigma$;
acoustic velocity	median $\pm 3\sigma$;
acoustic spectral width	median $\pm 3\sigma$;
acoustic SNR	above −25-dB threshold.

These limits were chosen from examination of the distributions of the respective parameters, from examination of large numbers of individual spectra, and from physical arguments. For example, the acoustic velocity estimate is not subject to any of the abovementioned errors except low return signal power. An unusually high clear-air SNR is probably due to a hard target (bird, insect, or aircraft), while an unusually low clear-air SNR is due to poor return signal power.

The statistical cleaning is not designed to deal with data contaminated by rain. The profiler responds very strongly to raindrops, and rain tends to occur over periods of at least several minutes. While horizontal wind measurements can be made with the 915-MHz profiler in stratiform rain, vertical wind and, therefore, flux measurements cannot be made. We therefore attempt to calculate the flux only during periods with no rain.

After cleaning, the time series of temperature is computed using both the acoustic and clear-air velocities using the standard RASS temperature retrieval equation,

$$T_v = (C_a - v_r)^2 \frac{M_d}{\gamma_d R}, \tag{2}$$

where C_a is the acoustic velocity, v_r is the clear-air radial velocity, M_d is the molecular weight of dry air, and γ_d is the ratio of specific heats for dry air. A linear trend is removed from the time series of temperature and radial wind. The heat flux is then calculated by the method of Peters et al. (1985):

$$Q_v = \rho \frac{C_p}{2} [\mathrm{cov}(T_v', w')(-1) + \mathrm{cov}(T_v', w')(1)], \tag{3}$$

where ρ is the air density, C_p is the heat capacity of air at constant pressure, and the argument of the covariance is the lag between the temperature and the vertical velocity. In this method, the correlation of temperature

TABLE 1. Characteristics of King Air flight legs.

Leg	Date	Start time (CST)	Duration (min)	Height (m AGL)
6D	18 June	1222	17	160
7A	20 June	0959	21	380
7B	20 June	1022	19	250
7C	20 June	1048	22	170
7D	20 June	1112	17	80
8A	21 June	0911	25	180
10A	23 June	0906	10	160
10B	23 June	1014	29	170

and vertical velocity is computed at plus and minus one lag, and these results are averaged to give the correlation estimate. The covariance at zero lag is not used, because it is contaminated by any errors that remain in the radial wind measurement, which enters into the temperature measurement as well in (2). The minimum fully resolvable scale in the along-wind direction is therefore twice the resolution cell size in that direction, or 160 m in the above example (2 m s^{-1} wind).

The 2-h averaging time was chosen as the longest possible time over which the atmosphere might be considered reasonably stationary. A flux estimate was made for each hour by overlapping the 2-h intervals.

c. *Aircraft data processing*

During the 18–25 June 1992 intensive period the NCAR King Air flew eight flight legs that met all the criteria for use in this study. The criteria were that the flight path was over the forest and site, the flight altitude was within the boundary layer, all necessary instruments were operating, and the leg length was at least 10 min (48 km along the flight track).

Data from each of the flight legs were checked at NCAR for gross sensor failure. We then carefully trimmed each leg to include only straight and level flight. The data were then extracted from the NCAR format at the 20-Hz rate. The Lyman-α hygrometer data were scaled to the chilled-mirror dewpoint instrument for each flight leg in order to eliminate flight-to-flight drift of the Lyman-α instrument (Friehe et al. 1986). For comparison with the profiler, the kinetic temperature, humidity, and vertical wind data were block-averaged to 1 s (approximately 80 m along the flight track.) A linear trend was removed and the virtual heat flux was then computed directly. Table 1 shows characteristics of the flight legs.

d. *Scaling*

Boundary-layer data are customarily presented in scaled form, that is, normalized to suitable combinations of variables in order to reduce scatter in the measurements and show fundamental relationships more clearly. In this case, a simple mixed-layer scaling (Stull 1988) was used. The virtual heat fluxes measured by the profiler–RASS (Q_{vp}) and the King Air (Q_{va}) were scaled to the surface virtual heat flux (Q_{vs}) measured by the sonic anemometer. In addition, the measurement heights were scaled to the boundary-layer height for some of the comparisons.

3. Results

a. *Individual day comparisons*

Table 2 compares the virtual heat flux from six flight legs to that measured by the profiler–RASS at the same time on the same day as the flight. The profiler–RASS flux is interpolated between adjacent 2-h averages. For statistical comparison, we use the relative difference, that is, the difference between the flux measured by the profiler–RASS and that measured by the aircraft normalized to the profiler measurement. The mean relative difference $[\overline{(Q_{vp} - Q_{va})/Q_{vp}}]$ is 0.27, where Q_v is virtual heat flux, subscript p is the profiler–RASS measurement, and subscript a is the aircraft measurement. The standard deviation of the relative difference is 0.18.

b. *Multiday average comparison at 150 and 250 m*

Figure 1 compares the virtual heat flux for five flight legs near 150 m above ground level (AGL) with the profiler–RASS virtual heat flux in the range gate centered at 150 m AGL averaged over the period 18–26 June. The fluxes are scaled to the surface flux. Each 1-h point of the profiler–RASS measurement is an average of the 2-h measurements centered at the indicated time for all days of the period on which surface data were available at that time. Therefore each point is an average over 5–7 days of 2-h measurements. The dotted lines are the $\pm 1\sigma$ sampling uncertainty (see below) for the profiler, and the vertical bars are the same for the aircraft legs.

Table 3 gives a numerical comparison of the five flight legs presented in Fig. 1 and one additional leg

TABLE 2. Virtual heat flux comparison with individual day profiler–RASS measurements; Q_v is virtual heat flux. Subscript p is profiler measurement and subscript a is King Air measurement. The difference and the absolute value of the relative difference (normalized to the prolifer flux) are also shown.

Leg	Q_{vp} (W m^{-2})	Q_{va} (W m^{-2})	$Q_{vp} - Q_{va}$ (W m^{-2})	$\left\lvert\frac{Q_{vp} - Q_{va}}{Q_{vp}}\right\rvert$
6D	120	103	17	0.14
7B	120	70	50	0.41
7C	100	100	0	0.00
8A	135	102	33	0.24
10A	125	63	62	0.49
10B	170	114	56	0.33

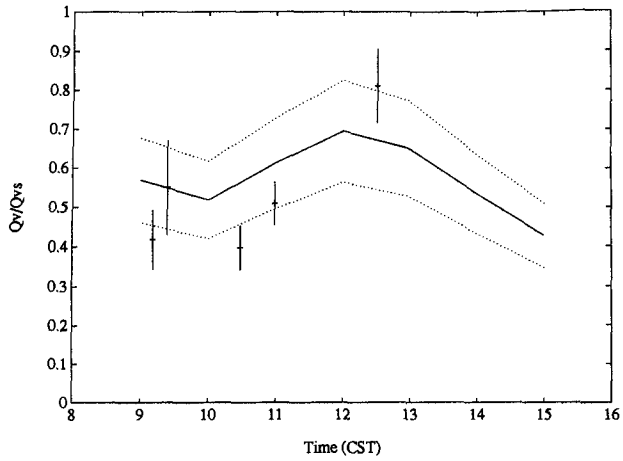

FIG. 1. Comparison of profiler–RASS 7-day average and King Air virtual heat flux measurements near 150 m AGL normalized to surface virtual heat flux. The solid line is the profiler–RASS measurement for 2-h periods centered around the indicated time, averaged over all days of the period 18–26 June for which surface data were available at that time. The dotted lines are the sampling uncertainty limits ($\pm 1\sigma$). The short horizontal lines are the virtual heat flux on scales longer than 1 s for the King Air flight legs, and the vertical bars are the sampling uncertainty limits ($\pm 1\sigma$).

TABLE 3. Scaled virtual heat flux comparison with 7-day average profiler–RASS measurements; Q_v is virtual heat flux. Subscript p is profiler measurement, subscript s is surface (sonic anemometer) measurement, and subscript a is King Air measurement. The difference and the absolute value of the relative difference (normalized to the profiler flux) are also shown.

Leg	$\frac{Q_{vp}}{Q_{vs}}$	$\frac{Q_{va}}{Q_{vs}}$	$\frac{Q_{vp}-Q_{va}}{Q_{vs}}$	$\left\lvert\frac{Q_{vp}-Q_{va}}{Q_{vp}}\right\rvert$
6D	0.66	0.81	−0.15	0.23
7B	0.58	0.38	0.20	0.34
7C	0.61	0.51	0.10	0.17
8A	0.55	0.55	0.00	0.00
10A	0.56	0.42	0.14	0.26
10B	0.56	0.40	0.16	0.29

(7B) at 250 m. The mean relative difference is 0.21 and the standard deviation of the relative difference is 0.12. Averaging the scaled profiler measurements thus reduces both the systematic and random differences with respect to the aircraft measurements.

In this presentation, no allowance is made for the differences in PBL height from day to day. This explains some of the observed scatter. Unfortunately, most of the flight legs were flown in the morning when the boundary-layer height was changing rapidly. The earliest leg, leg 10A, was also short, just under 10 min.

c. *Fitted profile comparison*

The canonical profile of virtual heat flux in the convective mixed layer below about $0.8z_i$, where z_i is the boundary-layer height, is a straight line when plotted versus z/z_i. This profile is seen in both observations (Stull 1988, 99–101) and models (Moeng 1984). Stull (1988, p. 370) proposes the relationship

$$\frac{Q_v}{Q_{vs}} = 1 - \alpha \frac{z}{z_i}, \qquad (4)$$

where α is a constant between 1.2 and 1.5.

The boundary-layer height z_i needed for scaling was determined from the profiler SNR (White et al. 1991a,b). The range-corrected SNR has a peak at the inversion, providing a continuous indication of boundary-layer height.

The measured profiles were determined by unweighted least-squares fitting. The relative height z/z_i was treated as the independent variable; that is, all uncertainty was attributed to the scaled flux measurement.

Figure 2 shows all 2-h-average profiler–RASS measurements below $0.8z_i$ during 18–26 June and the line fitted to them. As many as six profiler range gates are represented, depending on the PBL height. Measurements from 2-h averages centered at times from 0900 through 1200 CST are included, since these encompass the flight times used in the comparison. Figure 3 is the same presentation for the eight King Air flight legs in Table 1.

Figure 4 shows the same fitted lines from Figs. 2 and 3, with the addition of two lines from (4) with $\alpha = 1.2$ and $\alpha = 1.5$. The flux profiles measured by the profiler–RASS and the King Air are in good agreement. Both appear to underestimate the flux slightly with respect to the surface measurement. Alternatively, the surface flux could be in error.

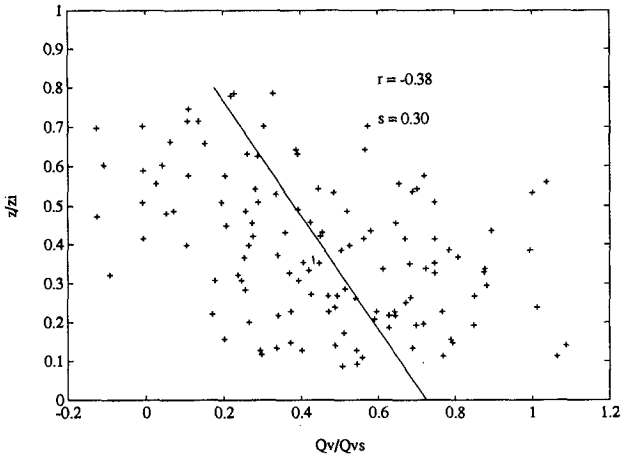

FIG. 2. Virtual heat flux measurements from the profiler–RASS for 2-h periods centered at each hour from 0900 to 1200 CST for the first six range gates. Only those measurements below $0.8z_i$ are shown. The line is the least-squares fit assigning all uncertainty to the flux, r is the correlation coefficient, and s is the standard deviation estimate of the fit.

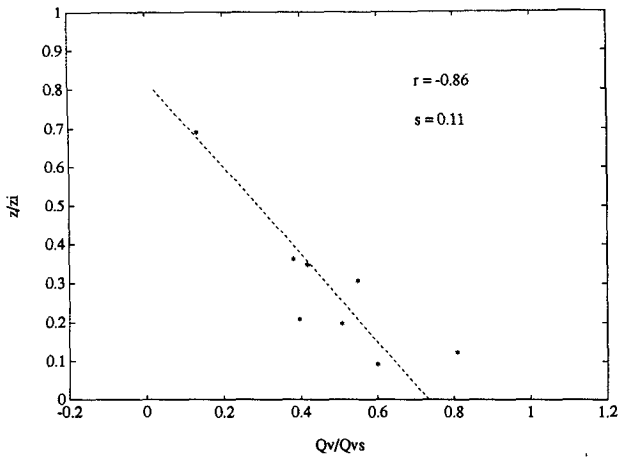

FIG. 3. Same as Fig. 3 but for eight King Air flight legs. Dashed line is the least-squares fit.

The correlation coefficients r and standard deviation estimates s are shown for the linear fits in Figs. 2 and 3. The correlation coefficient of -0.38 for the profiler–RASS fit is significant at a confidence level of more than 95%, and the coefficient of -0.86 for the aircraft fit is significant at a confidence level of 99%.

4. Discussion

The profiler–RASS technique measures virtual heat flux that agrees well with aircraft measurements and with a simple model (2). There is considerable scatter in the results, however, and there appear to be systematic differences between the profiler–RASS and aircraft measurements, and between those measurements and the surface flux measurements.

The two techniques sample the atmosphere very differently. The profiler–RASS samples a vertical stack of volumes directly over the site for a time period varying in these comparisons from 2 to 14 (noncontiguous) h. The aircraft samples a virtually one-dimensional path covering 50–100 km in 10–20 min. Both sampling methods have theoretical and practical problems. Under the light wind conditions present during this experiment, the profiler almost certainly does not sample a frozen turbulence field advected by the mean wind. Instead, it samples a turbulence field that is evolving on a time scale comparable to that for advection of large eddies. In addition, any tendency for thermals to form preferentially over terrain inhomogeneities will result in a flux measurement that is not representative of the area average flux. The aircraft flight path passes over terrain that differs from that around the profiler site, including occasional roads and buildings, bringing into question the representativeness of the aircraft measurement. The single-point surface flux measurement used for scaling also may not be representative of the area as a whole.

Time-average measurements such as those reported here are subject to considerable scatter because the energy-containing scales are large. An estimate of the uncertainty due to sampling for a finite time or distance is provided by the theoretical work of Wyngaard (1992) and the experiments of Lenschow and Stankov (1986). The estimate is based on the time or distance required for a time or distance average to converge to within a certain limit of the ensemble average. The relative uncertainty e (the standard deviation divided by the mean) is

$$e^2 = \frac{2F\tau}{t} \tag{5}$$

or

$$e^2 = \frac{2F\lambda}{L}, \tag{6}$$

where τ is the integral scale in time, λ is the integral scale in space of the flux, t is the sampling time, L the sampling distance, and

$$F = \frac{\overline{T_v'^2 w'^2} + (\overline{T_v' w'})^2}{(\overline{T_v' w'})^2}. \tag{7}$$

Lenschow and Stankov (1986) also investigated the integral scale for fluxes in the convective boundary layer and found the relation

$$\lambda = 0.16 z^{1/3} z_i^{2/3}. \tag{8}$$

Tables 4 and 5 give information about the expected uncertainty in these measurements calculated from the above relations. Table 4 shows the mean wind speed, normalized height, and variances of temperature and vertical wind observed on each flight leg. Table 5 shows the results of using those parameters to compute the integral scales in space (for the aircraft measurement

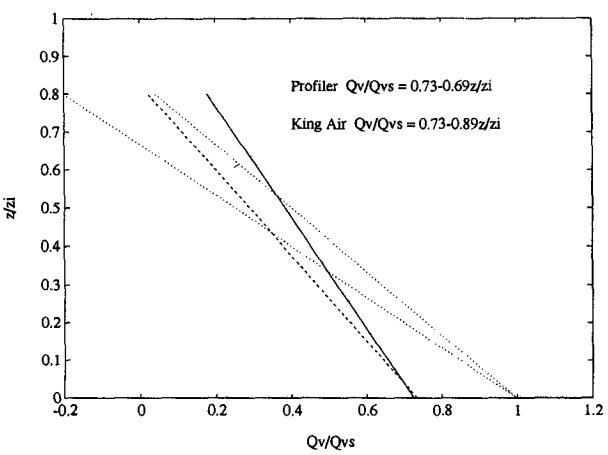

FIG. 4. The fitted lines for the profiler–RASS (Fig. 2, solid) and the King Air (Fig. 3, dashed) compared to Eq. (4) with $\alpha = 1.2$ and $\alpha = 1.5$ (dotted).

TABLE 4. Measured wind speed, height/PBL height, temperature variance, and vertical wind variance for King Air flight legs.

Leg	Wind speed ($m\ s^{-1}$)	$\frac{z}{z_i}$	$\overline{T_v^2}$	$\overline{w^2}$ ($m^2\ s^{-2}$)
6D	2.1	0.13	0.06	0.82
7B	2.0	0.36	0.09	0.81
7C	2.0	0.20	0.05	0.95
8A	4.9	0.31	0.37	0.85
10A	1.2	0.35	0.06	0.64
10B	0.7	0.21	0.19	1.19

itself) and in time (for the fixed profiler observation, assuming Taylor's hypothesis holds). Table 5 also shows the relative uncertainty expected for the aircraft leg and for a 2-h average profiler–RASS measurement. We note again that this is the relative uncertainty due to sampling of the turbulence, not including any contribution from instrumental errors.

Comparing the relative uncertainty estimates in Table 5 with the relative differences between the profiler–RASS flux and King Air measurements in Table 2 (individual day comparisons), we observe that the difference is less than the relative uncertainty for the profiler for all legs except 10A. There is a correlation between the differences and the uncertainty, legs with large uncertainties tending to have large differences. We therefore conclude that the random instrumental error in the profiler–RASS is less than the sampling uncertainty. The instrumental error is certainly less than 40% and probably less than 30% when averaged over 2 h.

Examining the multiday average comparisons (section 3b above and Fig. 1), we find that for the six flight legs in Tables 2, 3, 4, and 5, the mean integral scale in time is 48 s and the mean relative uncertainty is 0.16. Taking the profiler averaging time to be 14 h for the multiday average and applying (5) in the mean, the relative uncertainty for the profiler–RASS due to sampling is found to be 0.19. The standard deviation of the relative difference between the 7-day average profiler–RASS flux measurement and the flight legs is 0.12. This comparison also depends on the uncertainty of the surface flux measurement, which we estimate at 10%–20%. We therefore conclude that the random instrumental error in the profiler–RASS flux measurement is no more than 15% when averaged over 14 h.

The profiler–RASS measures 20%–35% more flux than the aircraft in the lowest two profiler range gates (150 and 250 m). When the measurements are scaled and extrapolated by least-squares fitting (Fig. 4) the profiler–RASS and aircraft profiles agree extremely well at the surface. The disagreement increases with height. The apparent systematic difference between the profiler–RASS flux measurement and the King Air measurement may be due to the differences in sampling (line versus volume, short versus long time, and horizontal inhomogeneity) mentioned above (Desjardins et al. 1992). Figure 5 shows the $\pm 1\sigma$ limits of the fits themselves, derived from the uncertainties of the slope and intercept. These fit uncertainties should not be confused with the uncertainty of the measurement. The substantial overlap of the $\pm 1\sigma$ uncertainties of the fit, even at the higher scaled heights, indicates that there is some probability that the profiles do not differ.

TABLE 5. Integral scales in space and time (using Taylor's hypothesis) and relative uncertainties ($\pm 1\sigma$) for King Air flight legs and surrounding profiler 2-h averages. Integral scales are computed from Eq. (8) and relative uncertainties are computed from Eqs. (5) and (6).

Leg	Integral scale in space λ (m)	Integral scale in time τ (s)	Relative uncertainty for flight leg	Relative uncertainty for profiler
6D	102	48	0.12	0.28
7B	80	40	0.20	0.49
7C	79	41	0.11	0.30
8A	65	13	0.22	0.41
10A	51	42	0.18	0.43
10B	76	102	0.14	0.69

The profiler–RASS and aircraft both measure less flux than the surface instrument (Fig. 4). The discrepancy is 27% of the surface value. Part of the discrepancy is accounted for by the scales measured. Flux on scales less than about 100 m is not measured by either the profiler–RASS or the comparable block-averaged aircraft results. If all available scales (up to 10 Hz) are retained in the aircraft measurement, the extrapolated value at the surface is increased from 0.73 to 0.84 (relative to the surface flux), so the neglect of small scales results in an approximately 15% underestimate. This is about half of the apparent discrepancy. The remain-

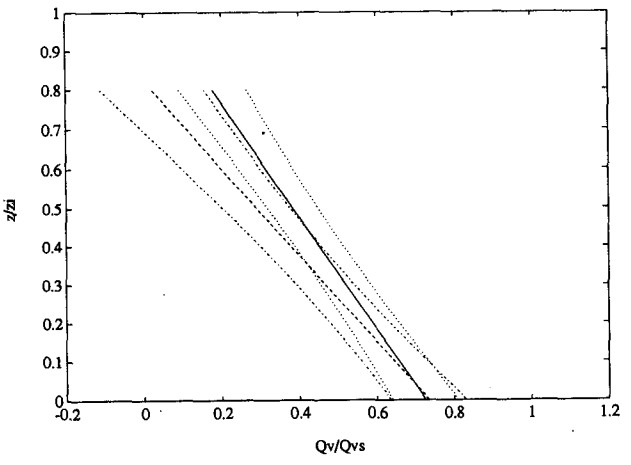

FIG. 5. The fitted lines with the $\pm 1\sigma$ uncertainties of the fits shown. These uncertainties were derived from the uncertainty of the slope and intercept of each fitted line. Solid: profiler–RASS fit (Fig. 2). Dashed: King Air fit (Fig. 3). Dotted: profiler–RASS fit uncertainty. Dash–dot: King Air fit uncertainty.

ing disagreement may again be due to sampling differences between the measurements, or to some other unknown cause.

A number of studies from the First ISLSCP (International Satellite Land Surface Climatology Project) Field Experiment (FIFE) relate to the comparison of aircraft and surface flux measurements. The FIFE experiment is comparable to the current study, having been conducted in a continental grassland. We emphasize sensible heat flux comparisons from FIFE, since they are most comparable to the virtual heat flux under discussion. Using sensible heat flux measurements from two aircraft, the National Research Council of Canada Twin Otter and the University of Wyoming King Air, Kelly et al. (1992) show a disagreement of 30% when extrapolated to the surface. The authors attribute half of the disagreement to undersampling of high frequencies. The cutoff frequencies were lower than those of the NCAR King Air, so this effect should be less important in the current study. Betts et al. (1992) compare a different set of fluxes measured by the Twin Otter during FIFE and find an 18% underestimate, which they explain by the undersampling of both high and very low frequencies. The FIFE studies used short (15 km) flight legs, while our current study uses much longer (50–100 km) legs, and we would not expect to be undersampling low frequencies. Another FIFE study by Grossman (1992) using the same NCAR King Air as the current study observed no systematic difference between the aircraft sensible or latent heat fluxes extrapolated to the surface and the fluxes measured at the surface, but only 2 days were studied. It is also worth noting that the surface flux measurements in FIFE were averages over a large number of sites and that the differences between individual sites were substantial (Smith et al. 1992). This is another indication that the single surface measurement site used in the current study may not be representative of the entire area.

5. Conclusions

We have shown that the boundary-layer profiler–RASS can measure virtual heat flux in the convective boundary layer and that the results are comparable to those from aircraft and theory. The measurement precision is limited primarily by practical considerations of averaging time, but even under light wind conditions a 2-h measurement can be sufficiently precise to be useful. Stronger winds would improve the accuracy by increasing the number of integral scales that could be averaged in a given time. The flux measurements can be made while the profiler is also producing standard wind and temperature profiles.

Acknowledgments. The surface data were graciously provided by Detleff Matt of NOAA Air Resources Laboratory, Atmospheric Turbulence and Diffusion Division, Oak Ridge, Tennessee. The members of the Tropical Dynamics and Climate Group of the NOAA Aeronomy Laboratory, under the direction of Ken Gage, assisted in the preparation of the profiler and in the analysis and discussion of the results. Tom VanZandt provided counsel on the manuscript. Jim Jordan of NOAA WPL helped set up the profiler–RASS and provided the clutter fence. Partial funding for this study was provided by the Department of Energy Atmospheric Radiation Measurement program. ROSE II was conducted in collaboration with the Southern Oxidant Study.

REFERENCES

Angevine, W. M., S. K. Avery, W. L. Ecklund, and D. A. Carter, 1993: Fluxes of heat and momentum measured with a boundary-layer wind profiler radar–radio acoustic sounding system. *J. Appl. Meteor.*, **32,** 73–80.

——, W. L. Ecklund, D. A. Carter, K. S. Gage, and K. P. Moran, 1994: Improved radio acoustic sounding techniques. *J. Atmos. Oceanic Technol.*, **11,** in press.

Betts, A. K., R. L. Desjardins, and J. I. MacPherson, 1992: Budget analysis of the boundary layer grid flights during FIFE 1987. *J. Geophys. Res.*, **97,** 18 533–18 546.

Desjardins, R. L., P. H. Schuepp, J. I. MacPherson, and D. J. Buckley, 1992: Spatial and temporal variations of the fluxes of carbon dioxide and sensible and latent heat over the FIFE site. *J. Geophys. Res.*, **97,** 18 467–18 476.

Ecklund, W. L., D. A. Carter, and B. B. Balsley, 1988: A UHF wind profiler for the boundary layer: Brief description and initial results. *J. Atmos. Oceanic Technol.*, **5,** 432–441.

Friehe, C. A., R. L. Grossman, and Y. Pann, 1986: Calibration of an airborne Lyman-alpha hygrometer and measurement of water vapor flux using a thermoelectric hygrometer. *J. Atmos. Oceanic Technol.*, **3,** 299–304.

Grossman, R. L., 1992: Convective boundary layer budgets of moisture and sensible heat over an unstressed prairie. *J. Geophys. Res.*, **97,** 18 425–18 438.

Kelly, R. D., E. A. Smith, and J. I. MacPherson, 1992: A comparison of surface sensible and latent heat fluxes from aircraft and surface measurements in FIFE 1987. *J. Geophys. Res.*, **97,** 18 445–18 454.

Lenschow, D. H., and B. B. Stankov, 1986: Length scales in the convective boundary layer. *J. Atmos. Sci.*, **43,** 1198–1209.

Matuura, N., Y. Masuda, H. Inuki, S. Kato, S. Fukao, T. Sato, and T. Tsuda, 1986: Radio acoustic measurement of temperature profile in the troposphere and stratosphere. *Nature,* **333,** 426–428.

May, P. T., R. G. Strauch, and K. P. Moran, 1988: The altitude coverage of temperature measurements using RASS with wind profiler radars. *Geophys. Res. Lett.*, **15,** 1381–1384.

——, ——, ——, and W. L. Ecklund, 1990: Temperature sounding by RASS with wind profiler radars: A preliminary study. *IEEE Trans. Geosci. Remote Sens.*, **28,** 19–28.

Moeng, C., 1984: A large-eddy-simulation model for the study of planetary boundary-layer turbulence. *J. Atmos. Sci.*, **41,** 2052–2062.

Peters, G., H. Hinzpeter, and G. Baumann, 1985: Measurements of heat flux in the atmospheric boundary layer by sodar and RASS: A first attempt. *Radio Sci.*, **6,** 1555–1564.

Smith, E. A., A. Y. Hsu, W. L. Crosson, R. T. Field, L. J. Fritschen, R. J. Gurney, E. T. Kanemasu, W. P. Kustas, D. Nie, W. J. Shuttleworth, J. B. Stewart, S. B. Verma, H. L. Weaver, and M. L. Wesely, 1992: Area-averaged surface fluxes and their time–space variability over the FIFE experimental domain. *J. Geophys. Res.*, **97,** 18 599–18 622.

Stull, R. B., 1988: *An Introduction to Boundary-Layer Meteorology.* Kluwer, 666 pp.

White, A. B., C. W. Fairall, and D. W. Thompson, 1991a: Radar observations of humidity variability in and above the marine atmospheric boundary layer. *J. Atmos. Oceanic Technol.*, **8,** 639–658.

——, ——, and D. E. Wolfe, 1991b: Use of 915 Mhz wind profiler data to describe the diurnal variability of the mixed layer. Preprints, *Seventh Joint Conf. on Applications of Air Pollution Meteorology with AWMA,* Amer. Meteor. Soc.,

Wyngaard, J. C., 1992: Atmospheric turbulence. *Ann. Rev. Fluid Mech.*, **24,** 205–233.